J. Fluid Mech. (1989), *vol.* 206, *pp.* 463–475
Printed in Great Britain

Aerodynamic characteristics of a two-dimensional porous sail

By S. MURATA AND S. TANAKA
Toyota Technological Institute, 2–12 Hisakata, Tempaku, Nagoya, 468 Japan

(Received 1 August 1988 and in revised form 14 March 1989)

A method is presented for the numerical analysis of the aerodynamic characteristics of a two-dimensional single-surface porous sail. In this analysis the authors apply a series of Jacobi polynomials to express the pressure distribution and chordwise shape, considering carefully leading-edge conditions. It is found that the aerodynamic stability of a sail increases with increasing porosity. The effects of porosity on the value of the life coefficient and the position of the centre of pressure are shown in diagrams as functions of angle of attack and of excess length of membrane over the chord length.

1. Introduction

Single-surface flexible sails are used on yachts, sail-boards, hang gliders, motor gliders and various wind turbines owing to their low cost and light weight as well as simplicity of construction. Hence it is worthwhile to study their aerodynamic behaviour experimentally as well as theoretically.

For a non-porous membrane, an analytical investigation of the characteristics of a sail has been the subject of a number of previous studies. Voelz (1950), Thwaites (1961) and Nielsen (1963) studied the two-dimensional incompressible inviscid flow past a sail utilizing thin-aerofoil theory assuming that the angle of attack α is small. Recently, Murai & Maruyama (1982) studied the same problem in more detail by taking into account the effects of an elastically supported trailing edge.

For finite α, Vanden-Broeck (1982) developed a nonlinear computational method and Sneyd (1984) studied the influence of membrane extensibility on sail characteristics.

However, very few experiments have been made on non-porous single-surface sails. Nielsen (1963) summarized some experimental results and showed that the lift curve slope, but not the lift itself, agrees with a linear theory for an excess length ratio smaller than 0.06 and the position of the centre of pressure is in good agreement with his theory for cambers less than 15%. Recently, another experimental study was done on a quasi two-dimensional, single-surface sail with small camber at small incidence by Newman & Low (1984). One of their conclusions is that near zero incidence the values of lift and tension of a sail lie between the conventional linearized theory and a modified theory proposed by them.

The facts described above show that linearized theory is still useful for the evaluation of experimental data and the prediction of aerodynamic behaviour.

One of the problems raised in the analytical studies by Thwaites and Nielsen was the question of the influences of porosity on the aerodynamic characteristics of a sail. To the knowledge of the authors only the pioneering work of Barakat (1968) studies a porous sail, although there are many studies of non-porous sails. He proposed a

method to calculate numerically the aerodynamic behaviour of porous sails by applying Jacobi polynomials.

In this paper the authors have improved his method to achieve better accuracy by expressing the aerodynamic coefficients in a simpler form. The important aerodynamic behaviour associated with the influence of porosity on the stability of the sail, on the value of the lift coefficient and on the position of the centre of pressure are thus clarified.

2. Basic equations

As shown in figure 1, the chordwise shape consists of a strip of sail stretched between the leading edge ($X = -c$, $Y = 0$) and the trailing edge ($X = c$, $Y = 0$). It is positioned in a uniform flow of speed U, which is inclined at an angle of attack α to the X-axis. In inviscid flow, the membrane tension T is constant over the camber line, although it decreases slightly from the leading edge to the trailing edge in real flow owing to the skin friction. The pressure difference across the membrane is

$$\Delta p = -T\frac{\mathrm{d}^2 Y}{\mathrm{d}X^2} \tag{1}$$

because the slope of the sail is small.

If the density of fluid is denoted by ρ, the lift on the sail element $\mathrm{d}X$ is $\rho U\gamma(X)\,\mathrm{d}X$ and the pressure difference is given by

$$\Delta p = \rho U\gamma(X), \tag{2}$$

where $\gamma(X)$ is the strength of the vortex sheet per unit length distributed in $-c \leqslant X \leqslant c$, $Y = 0$, which represents the sail in linearized theory.

The speed of through-flow due to the porosity of the sail may be taken to be proportional to Δp, and hence to $\gamma(X)$. Now we define a coefficient k in such a manner that the speed of through-flow in the Y-direction is $k\gamma(X)$. The inclination of the flow speed at the sail surface to the X-axis is $(Y' + k\gamma(X)/U)$, and this must be equal to the inclination of the flow speed which is the sum of the main flow speed and the speed induced by the vortex sheet, namely,

$$\alpha + \frac{1}{2\pi U}\int_{-c}^{c} \gamma(X_0)\,(X_0 - X)^{-1}\,\mathrm{d}X_0.$$

Thus we have Thwaites' equation:

$$-\frac{1}{2\pi}\int_{-c}^{c}\frac{\gamma(X_0)}{X_0 - X}\,\mathrm{d}X_0 = U\alpha - UY' - k\gamma(X). \tag{3}$$

In this study, we assume that the sail has a constant porosity coefficient k along the camber line.

Let us change the variables X, Y to normalized ones x, y defined by $X = cx$, $Y = cy$ and put

$$\bar{\gamma}(x) = \frac{p(x)}{\rho U^2} = \frac{\gamma(x)}{U}, \tag{4}$$

$$\bar{T} = \frac{T}{\rho U^2}, \tag{5}$$

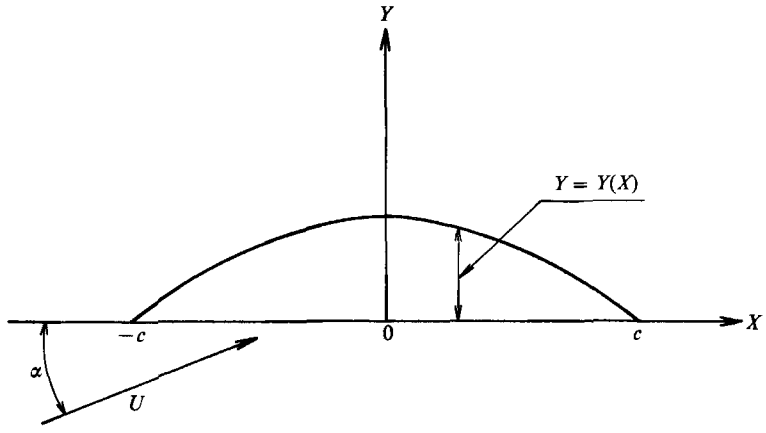

FIGURE 1. Axes and notation.

where $\bar{\gamma}(x)$ is the normalized vortex distributions and $\bar{T}$ is a tension coefficient. Thus the normalized versions of (3) and (1) are

$$k\bar{\gamma}(x)-\frac{1}{2\pi}\int_{-1}^{1}\frac{\bar{\gamma}(x_0)}{x_0-x}\mathrm{d}x_0=\alpha-\frac{\mathrm{d}y}{\mathrm{d}x}=-F(x), \tag{6}$$

$$-\bar{T}\frac{\mathrm{d}}{\mathrm{d}x}F(x)=\bar{\gamma}(x). \tag{7}$$

Equation (6) is a singular integral equation with a kernel of Cauchy type, and the inclusion of porosity leads to a Fredholm integral equation of the second kind, whereas an integral equation of the first kind is encountered in the usual impermeable case.

The length of the membrane is evaluated as follows:

$$l=\int_{-c}^{c}(1+Y'^2)^{\frac{1}{2}}\mathrm{d}X,$$

where $Y'=\mathrm{d}Y/\mathrm{d}X$. For a small slope, the length l can be written in the form

$$l=2c+\frac{1}{2}\int_{-c}^{c}Y'^2\mathrm{d}X. \tag{8}$$

For a real sail, an angle of attack α and an excess length ratio $\delta=(l-2c)/2c$ are given and the tension coefficient $\bar{T}$ is an unknown variable. But here we solve (6) and (7) for given values of α and $\bar{T}$, and compute δ from (8).

3. Solution of the basic equations

Erdogan, Gupta & Cook (1973) showed that the explicit solution of (6) is

$$(k^2+0.25)\,\bar{\gamma}(x)=-kF(x)+\frac{1}{2\pi}(1-x)^{\beta}(1+x)^{\sigma-\beta}\int_{-1}^{1}\frac{F(x_0)\,\mathrm{d}x_0}{(1-x_0)^{\beta}(1+x_0)^{\sigma-\beta}(x-x_0)}, \tag{9}$$

where

$$\cot(\beta\pi)=2k. \tag{10}$$

The exponent β, which characterizes the singularity at the leading edge, depends on the porosity k as shown in (10), and diminishes with an increase in porosity. As the

porosity decreases to zero, a square-root singularity ($\beta = \frac{1}{2}$) at the leading edge, which is a feature of the impermeable sail, appears. The exponent σ must be equal to 0, 1 or -1. But for $\sigma = -1$, the solution does not satisfy the Kutta condition. The solution for $\sigma = 1$ has no singularity at the leading edge and the trailing edge, and this solution, which represents the flow at zero incidence, exists only when the following condition is satisfied:

$$\int_{-1}^{1} \frac{F(t)\,\mathrm{d}t}{(1-t)^{\beta}(1+t)^{1-\beta}} = 0. \tag{11}$$

The solution (9) for $\sigma = 0$ can be applied in every case when the Kutta condition is satisfied. Barakat (1968) applied this type of solution and expressed the vortex distribution as follows:

$$\bar{\gamma}(x) = \left(\frac{1-x}{1+x}\right)^{\beta} \sum_{n=1}^{m} A_n P_n^{(\beta,-\beta)}(x), \tag{12}$$

where $P_n^{(\beta,-\beta)}(x)$ is Jacobi polynomial.

Combining the solution (9) for $\sigma = 1$ with that for $\sigma = 0$, Nielsen (1963) expressed the vortex distribution over the non-porous sail ($k = 0$) by utilizing a Glauert series in the form

$$\bar{\gamma}(x) = C\cot(\tfrac{1}{2}\theta) + \sum_{n=1}^{m} A_n \sin(n\theta), \tag{13}$$

where $$x = \cos\theta.$$

In (13), the vortex distribution

$$\bar{\gamma}(x) = C\cot(\tfrac{1}{2}\theta)$$

is the solution (9) when $k = 0$, $F(x_0) = C$ and $\sigma = 0$, which is the vortex distribution on a flat plate with an angle of attack C. For $C = 0$, (13) becomes

$$\bar{\gamma}(x) = \sum_{n=1}^{m} A_n \sin(n\theta),$$

which expresses the vortex distribution at zero incidence. The Glauert series (13) expresses the part of the vortex distribution with leading-edge singularity and the non-singular part separately. The employment of this series makes it possible to express the aerodynamic coefficients of a sail by only the first three coefficients of (13), and makes the calculation accuracy better.

For a porous sail, the same type of solution (9) as Nielsen's can be used:

$$\begin{aligned}(k^2+0.25)\,\bar{\gamma}(x) = -kF(x) &+ \frac{1}{2\pi}\left(\frac{1-x}{1+x}\right)^{\beta} \int_{-1}^{1} \left(\frac{1+x_0}{1-x_0}\right)^{\beta} \frac{C}{x-x_0}\,\mathrm{d}x_0 \\ &+ \frac{(1-x)^{\beta}(1+x)^{1-\beta}}{2\pi} \int_{-1}^{1} \frac{\{F(x_0)-C\}\,\mathrm{d}x_0}{(1-x_0)^{\beta}(1+x_0)^{1-\beta}(x-x_0)},\end{aligned} \tag{14}$$

where C is determined from the following relation:

$$\int_{-1}^{1} \frac{\{F(x_0)-C\}\,\mathrm{d}x_0}{(1-x_0)^{\beta}(1+x_0)^{1-\beta}} = 0. \tag{15}$$

Let us express the slope of the sail y' in a series of Jacobi polynomials $P_n^{(-\beta,\beta-1)}(x)$, which has the weight function $(1-x)^{-\beta}(1+x)^{\beta-1}$, as follows:

$$y' = \alpha + F(x) = A_0 + \sum_{n=1}^{m} A_n P_n^{(-\beta,\beta-1)}(x). \tag{16}$$

When $C = A_0 - \alpha$, that is when

$$F(x) - C = \sum_{n=1}^{m} A_n P_n^{(-\beta,\beta-1)}(x)$$

the condition (15) is satisfied. Thus the constant C is determined. Substituting (16) into (14) we obtain

$$\bar{\gamma}(x) = \frac{1}{(k^2+0.25)}\left\{\frac{(A_0-\alpha)}{2\sin(\beta\pi)}\left(\frac{1-x}{1+x}\right)^{\beta} + \frac{(1-x)^{\beta}(1+x)^{1-\beta}}{4\sin(\beta\pi)}\sum_{n=1}^{m} A_n P_n^{(\beta,1-\beta)}(x)\right\}. \quad (17)$$

In the above procedure, we utilize the following formulae (Gradshteyn & Ryzhik 1980):

$$\frac{1}{\pi}\int_{-1}^{1} \frac{P_n^{(-\beta,\beta-1)}(x_0)\,\mathrm{d}x_0}{(1-x_0)^{\beta}(1+x_0)^{1-\beta}(x-x_0)} = 2k\frac{P_n^{(-\beta,\beta-1)}(x)}{(1-x)^{\beta}(1+x)^{1-\beta}} + \frac{P_{n-1}^{(\beta,1-\beta)}(x)}{2\sin(\beta\pi)}, \quad (18)$$

$$\frac{1}{\pi}\int_{-1}^{1}\left(\frac{1+x_0}{1-x_0}\right)^{\beta}\frac{\mathrm{d}x_0}{x-x_0} = -\frac{1}{\sin(\beta\pi)} + 2k\left(\frac{1+x}{1-x}\right)^{\beta}. \quad (19)$$

The first term in the right-hand side of (17) represents the vortex distribution on a porous flat plate at an angle of attack $\alpha - A_0$.

Substitution of (16) and (17) into (7) and utilization of the following formula:

$$2\frac{\mathrm{d}}{\mathrm{d}x}\{P_n^{(-\beta,\beta-1)}(x)\} = nP_{n-1}^{(1-\beta,\beta)}(x), \quad (20)$$

lead to the final form of the equation, namely

$$-\bar{T}\sum_{n=1}^{m} nA_n P_{n-1}^{(1-\beta,\beta)}(x) = \frac{1}{(k^2+0.25)\sin(\beta\pi)}\left\{(\alpha-A_0)\left(\frac{1-x}{1+x}\right)^{\beta} - \frac{(1-x)^{\beta}(1+x)^{1-\beta}}{2}\sum_{n=1}^{m} A_n P_{n-1}^{(\beta,1-\beta)}(x)\right\}. \quad (21)$$

By making use of the relation

$$P_{n-1}^{(\beta,1-\beta)}(x) = (-1)^n P_n^{(1-\beta,\beta)}(-x) \quad (22)$$

we can express (21) by only one kind of Jacobi polynomial, $P_{n-1}^{(\beta,1-\beta)}(x)$.

Because of the geometrical constraint that the leading and the trailing edges of the sail lie on the X-axis, we have

$$y(1) = y(-1) = 0.$$

Taking account of (16), we obtain the following relations.

$$\left.\begin{aligned} \int_{-1}^{1} y'\,\mathrm{d}x = 2A_0 + \sum_{n=1}^{m} A_n \int_{-1}^{1} P_n^{(-\beta,\beta-1)}(x)\,\mathrm{d}x = 0, \\ A_0 = -\frac{1}{2}\sum_{n=1}^{m} A_n \int_{-1}^{1} P_n^{(-\beta,\beta-1)}(x)\,\mathrm{d}x. \end{aligned}\right\} \quad (23)$$

The procedure for the numerical calculation of (21) is as follows. In order to minimize the numerical error, the zero points of Jacobi polynomials $P_m^{(\beta,\beta-1)}(x)$ are selected as matching points, where (21) is satisfied. The first approximate coordinates of the zero points of the Jacobi polynomials are given by

$$x_{s,1} = \cos\left\{\frac{2\beta-1+4s}{4(m+1)}\pi\right\}. \quad (24)$$

In order to calculate more accurately the coordinates of the zero points, Newton's successive method is adopted, namely

$$x_{s,n} = x_{s,n-1} - \frac{P_m^{(\beta,1-\beta)}(x_{s,n-1})}{\frac{\mathrm{d}}{\mathrm{d}x}\{P_m^{(\beta,\beta-1)}(x_{s,n-1})\}}. \tag{25}$$

The derivative $\mathrm{d}\{P_m^{(\beta,1-\beta)}(x)\}/\mathrm{d}x$ is evaluated from

$$(1-x^2)\frac{\mathrm{d}}{\mathrm{d}x}\{P_m^{(\beta,1-\beta)}(x)\} = -m\left(x+\frac{2\beta-1}{2m+1}\right)P_m^{(\beta,1-\beta)}(x) + \frac{2(\beta+m)(m+1-\beta)}{(2m+1)}P_{m-1}^{(\beta,1-\beta)}(x). \tag{26}$$

The Jacobi polynomial $P_m^{(\beta,1-\beta)}(x)$ is calculated from the recurrence formulae.

Once the coefficients A_n have been calculated for a specified k and $\bar{T}$ from (21), we can utilize (16) and (17) to determine the sail shape and the vortex distribution on the sail.

4. Eigenvalue problem

Nielsen discussed the eigenvalue problem at zero incidence and reached the conclusion that the eigenvectors are partitioned into two independent sets: one is an even function and the other is an odd function. Then he discussed their characteristics in detail. When we consider the case of zero incidence and set $\alpha - A_0 = 0$ in (21), we obtain the same results as Nielsen's. But the odd set is physically meaningless since components of eigenvectors A_n are determined from α because $A_0 (= \alpha)$ is not zero. In order to obtain physically meaningful eigenvectors, we have to set $\alpha = 0$ in (21), which then becomes

$$\left.\begin{aligned} &(\bar{T}\boldsymbol{B} - \boldsymbol{D})\,\boldsymbol{A} = 0, \\ &b_{ij} = jP_{j-1}^{(1-\beta,\beta)}(x_i), \\ &d_{ij} = \frac{1}{2(k^2+0.25)\sin(\beta\pi)}\left\{(1-x_i)^{\beta}(1+x_i)^{1-\beta}P_{j-1}^{(\beta,1-\beta)}(x_i) \right. \\ &\qquad\qquad \left. -\left(\frac{1-x_i}{1+x_i}\right)^{\beta}\int_{-1}^{1} P_j^{(-\beta,\beta-1)}(x)\,\mathrm{d}x\right\}, \end{aligned}\right\} \tag{27}$$

where $\boldsymbol{B}$ and $\boldsymbol{D}$ are matrices with components b_{ij} and d_{ij} respectively and $\boldsymbol{A}$ is a vector with components A_n. In order to estimate eigenvalues and eigenvectors, we employed the following procedure. Calculating the inverse matrix $\boldsymbol{B}^{-1}$ by Gauss's elimination method and multiplying both sides of (27) by $\boldsymbol{B}^{-1}$, we can obtain the eigenvalues and the eigenvectors by the power method and the Hotteling method.

When the numbers m of matching points are 7, 9, 11 and 30 the values of maximum tension eigenvalues $\bar{T}_1$ are 1.72748, 1.72746, 1.72745 and 1.72745, respectively. This result shows that $\bar{T}_1$ can be estimated with a satisfactory accuracy when we put $m = 11$. Therefore all calculations in this paper were performed by setting $m = 11$.

For the non-porous sail, the tension eigenvalues calculated from the present method by setting $\alpha - A_0 = 0$ are

$$\bar{T}_1 = 1.7275, \quad \bar{T}_2 = 0.7260, \quad \bar{T}_3 = 0.4634,$$

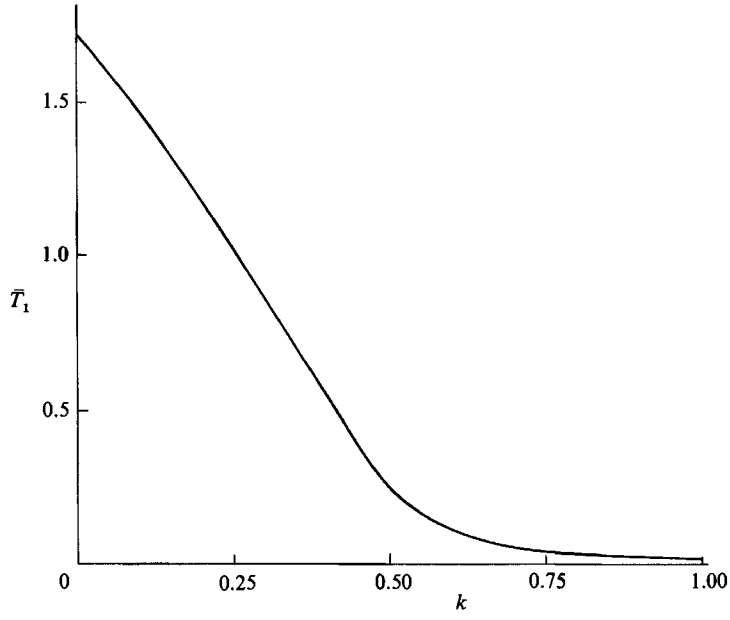

FIGURE 2. Maximum tension eigenvalues.

which coincide with Nielsen's results with an error of 0.02%, while the tension eigenvalues given by Barakat are

$$\bar{T}_1 = 1.7241, \quad \bar{T}_2 = 0.7262, \quad \bar{T}_3 = 0.3396.$$

There is a large difference in the third eigenvalue $\bar{T}_3$ between the present method and Barakat's.

Since α is not zero when $\bar{T}_2$ is 0.7260, this eigenvalue is physically meaningless. Putting $\alpha = 0$, we obtain another meaningful eigenvalue

$$\bar{T}_2 = 0.5563$$

which coincides with Murai & Maruyama's result with a satisfactory accuracy.

For a porous sail, the maximum eigenvalues $\bar{T}_1$ calculated from the double QR method are shown in figure 2. They coincide graphically with the values calculated by Barakat for $k \leqslant 0.4$. As an example, for the value of $\bar{T}_1$ when k is 0.4 Barakat obtained 0.5797, while the present authors obtained 0.5741. From figure 2, it is seen that the eigenvalue $\bar{T}_1$ diminishes with an increase in k. From the viewpoint of the value of $\bar{T}_1$, which is the criterion of stability when a sail with constant tension is examined, the stability increases with rising porosity. For $k \geqslant 0.2753$, all the values of $\bar{T}_n (n \neq 1)$ are complex numbers.

5. Sail characteristics

Since the basic equation (21) is of the linear type, coefficients A_n are proportional to the angle of attack α. It is clear that the slope y' is proportional to A_n from (16) and the excess length ratio δ is also proportional to A_n^2 from (8). Therefore, y is

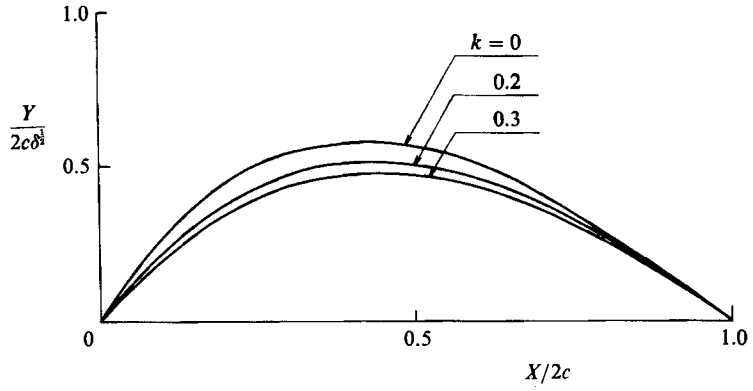

FIGURE 3. Shapes of sail for various values of porosity. $\bar{T} = 10$.

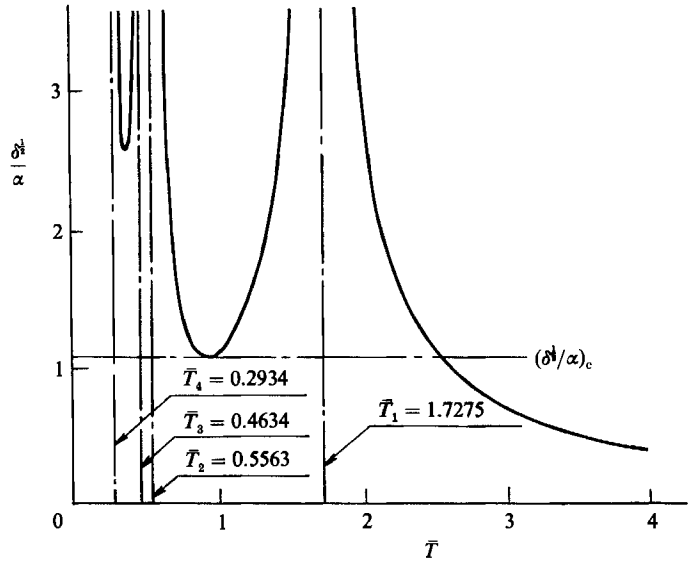

FIGURE 4. Excess length ratio ($k = 0$).

proportional to $\delta^{\frac{1}{2}}$. When $k = 0$ and $\bar{T} = 10$ the values of $Y/2c\delta^{\frac{1}{2}}$ calculated from the present method coincide with Nielsen's within an error of 0.02%, but are different by 2% from Barakat's values. For various values of porosity k, the shapes of a wing sail for $\bar{T} = 10$ are shown in figure 3.

In figures 4 and 5, the values of $\delta^{\frac{1}{2}}/\alpha$ calculated from (8) are plotted versus the tension coefficient $\bar{T}$ for various values of k. When $\delta^{\frac{1}{2}}/\alpha \geqslant (\delta^{\frac{1}{2}}/\alpha)_c$, various modes of sail shape appear as shown in figure 6. In order to illustrate the relation between $(\delta^{\frac{1}{2}}/\alpha)_c$ and porosity k, figure 7 has been prepared. From this figure, it is clear that an increase in porosity increases $(\delta^{\frac{1}{2}}/\alpha)_c$, which is the criterion of stability when 'looseness' or excess length is considered. Figure 8 shows the relation between $\delta^{\frac{1}{2}}/\alpha$ and $\bar{T}$ for various values of $k(\geqslant 0.3)$.

In the usual manner of linearized theory, the lift coefficient C_L can be obtained from integration of the pressure difference $\bar{\gamma}(x)$, and the moment coefficient C_M is

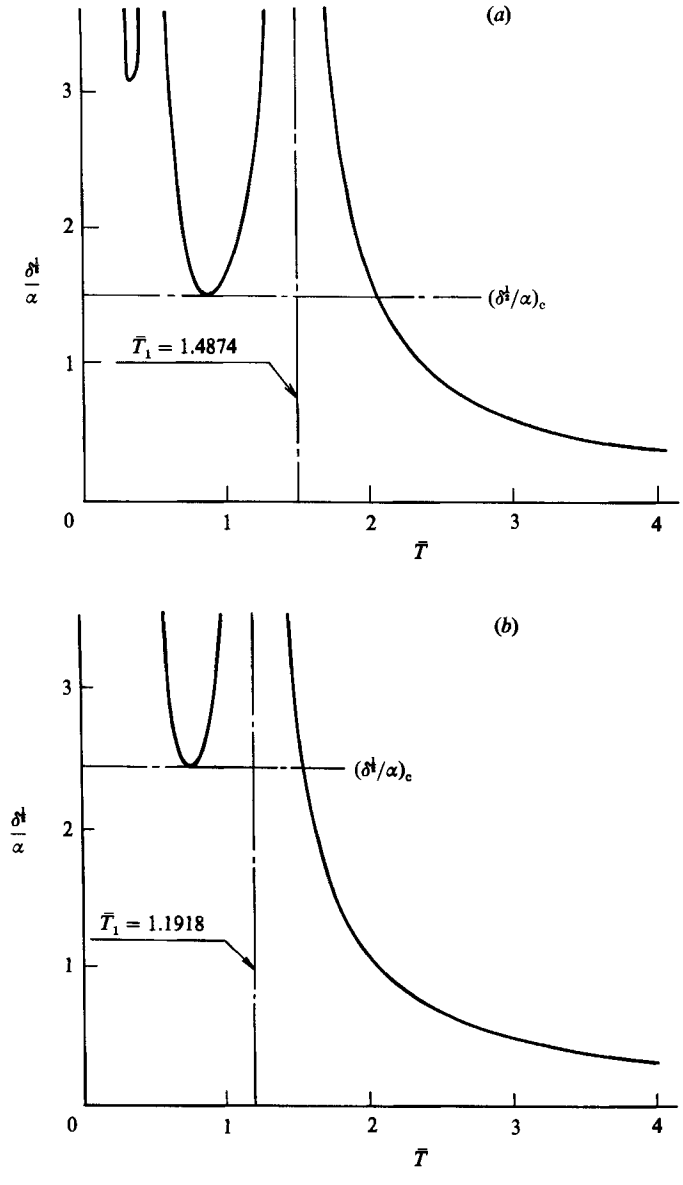

FIGURE 5. Excess length ratio. (*a*) $k = 0.1$; (*b*) $k = 0.2$.

obtained by integrating the product of $\bar{\gamma}(x)$ and the coordinate x over the chord. Integration of the first term in the right-hand side of (17) yields

$$C_{L0} = -(A_0 - \alpha)\frac{\beta\pi}{(k^2+0.25)\{\sin(\beta\pi)\}^2}, \tag{28}$$

$$C_{M0} = (A_0 - \alpha)\frac{\beta^2\pi}{(k^2+0.25)\{\sin(\beta\pi)\}^2}, \tag{29}$$

which give the lift and the moment coefficients for a porous flat plate when we put $A_0 = 0$.

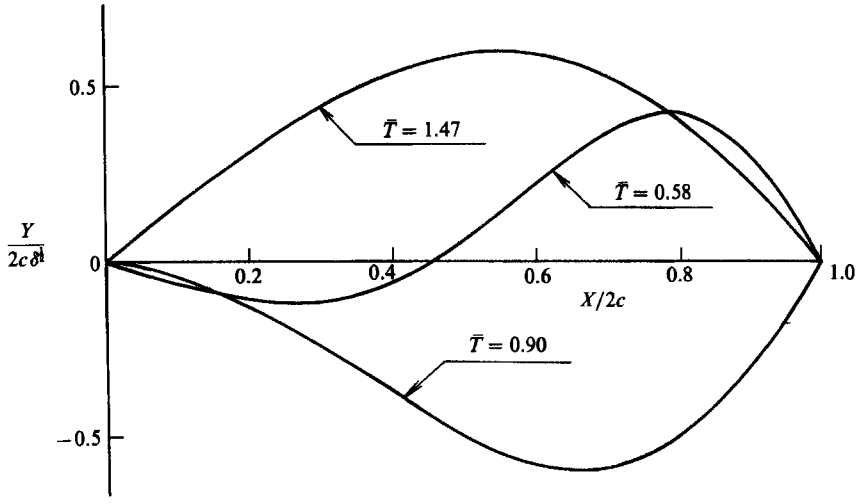

FIGURE 6. Various shapes of sail in the supercritical region: $k = 0.2$, $\delta^{\frac{1}{2}}/\alpha = 3$.

To prepare the necessary formulae to integrate the second term in the right-hand side of (17), we utilize the orthogonal characteristics of Jacobi polynomials and consider the relations

$$P_0^{(\beta,1-\beta)}(x) = 1, \quad P_1^{(\beta,1-\beta)}(x) = x. \tag{30}$$

Thus we obtain

$$\int_{-1}^{1} (1-x)^{\beta}(1+x)^{1-\beta} P_n^{(\beta,1-\beta)}(x)\,\mathrm{d}x = \begin{Bmatrix} 0 & (n \neq 0) \\ 2\beta(1-\beta)\pi/\sin(\beta\pi) & (n = 0), \end{Bmatrix} \tag{31}$$

$$\int_{-1}^{1} x(1-x)^{\beta}(1+x)^{1-\beta} P_n^{(\beta,1-\beta)}(x)\,\mathrm{d}x = \begin{Bmatrix} 0 & (n \neq 0, 1) \\ \dfrac{2(1-2\beta)\beta(1-\beta)\,\pi}{3\sin(\beta\pi)} & (n = 0) \\ \dfrac{\beta(\beta+1)\,(2-\beta)(1-\beta)\,\pi}{3\sin(\beta\pi)} & (n = 1). \end{Bmatrix} \tag{32}$$

Making use of the above formulae, we find that

$$C_L = \frac{\beta\pi}{(k^2+0.25)\{\sin(\beta\pi)\}^2}\{(\alpha - A_0) - \tfrac{1}{2}A_1(1-\beta)\}, \tag{33}$$

$$C_M = \frac{\beta\pi}{(k^2+0.25)\{\sin(\beta\pi)\}^2}\left[-\beta(\alpha - A_0) - \frac{1-\beta}{12}\{2(1-2\beta)A_1 + (\beta+1)(2-\beta)A_2\}\right] \tag{34}$$

Then the position of the centre of pressure is given by

$$C_P = \tfrac{1}{2}(1 + C_M/C_L). \tag{35}$$

The series of Jacobi polynomials (16) used to show the slope of the sail make it possible to express the lift and the moment coefficients and the position of the centre of pressure by their first three coefficients as shown in (33)–(35) in the same manner as in the Glauert's series employed by Nielsen.

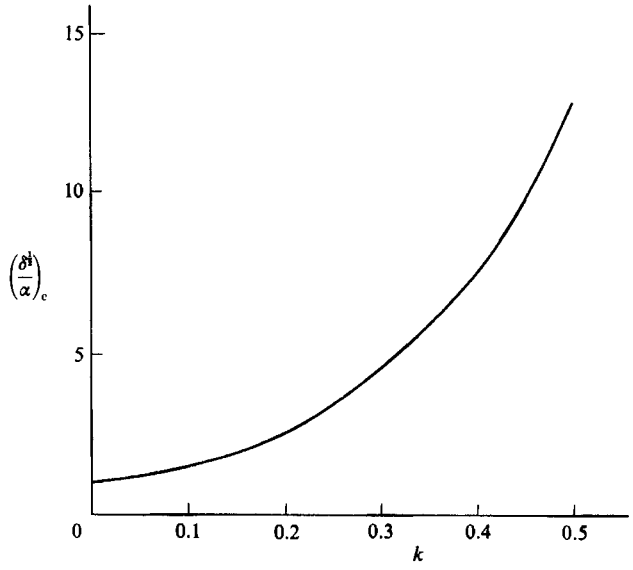

FIGURE 7. Critical excess length.

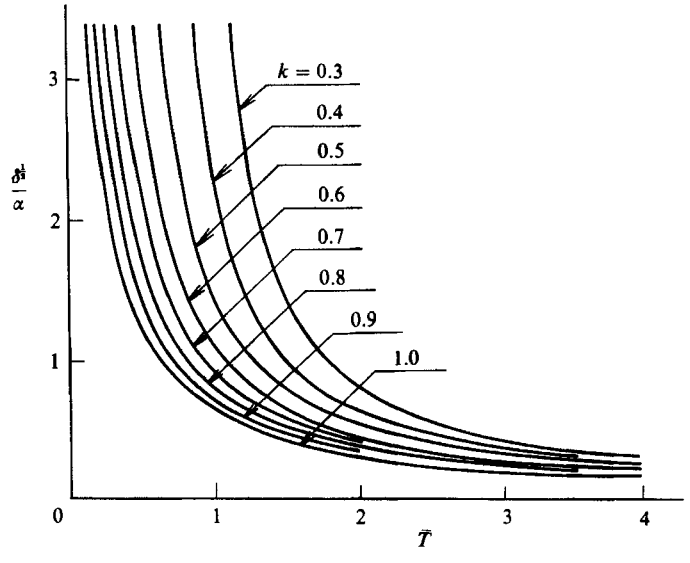

FIGURE 8. Excess length ratio ($k \geqslant 0.3$).

From figure 9 it is seen that an increase in porosity k and a decrease in excess length ratio $\delta^{\frac{1}{2}}/\alpha$ lead to a decrease in the lift coefficient slope C_L/α. Figure 10 shows the graph of C_P against $\delta^{\frac{1}{2}}/\alpha$ for various values of k. The centre of pressure approaches the trailing edge when the porosity of the sail increases. In figures 9 and 10, solid lines show the values when only one model of the sail shape appears, and dotted lines show the values at a tension coefficient larger than the maximum tension eigenvalue for various modes.

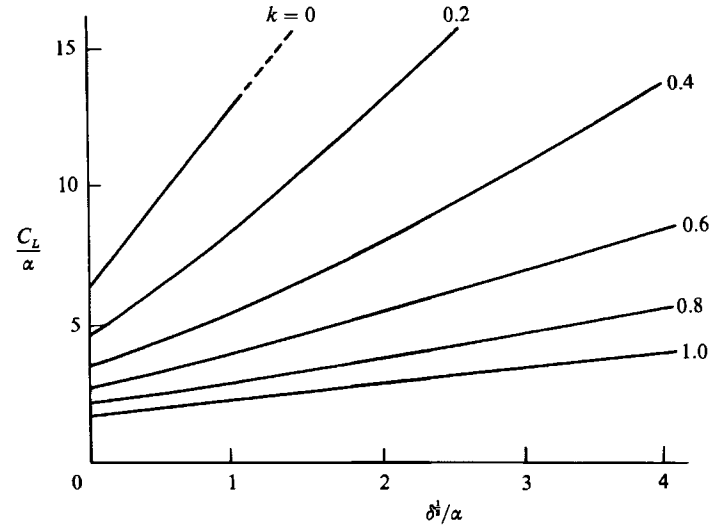

FIGURE 9. Lift characteristics.

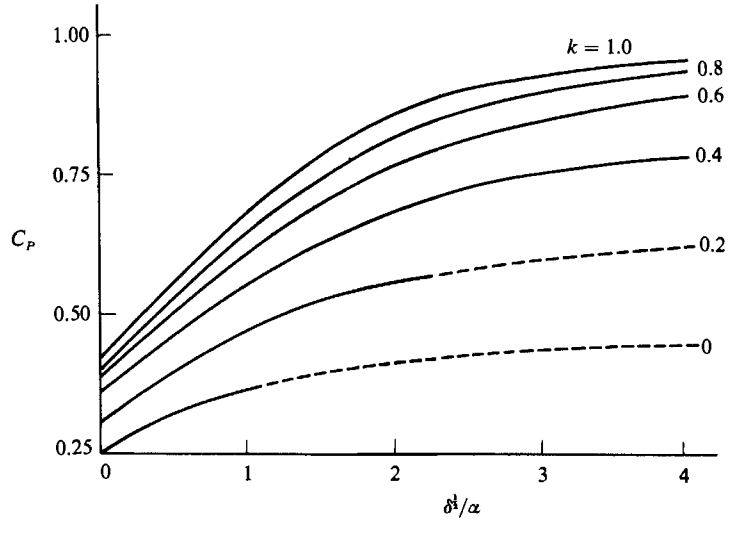

FIGURE 10. Centre of pressure.

6. Conclusions

In the present paper the authors have improved Barakat's method of numerical calculation of the aerodynamic coefficients and thereby improved the calculation accuracy. The results of a numerical analysis show that good stability characteristics from the viewpoints of the value of maximum tension eigenvalue and critical excess length ratio, can be obtained when the porosity of the membrane is high. With an increase in porosity and a decrease in excess length, the slope of the lift coefficient curve decreases as shown in figure 9. The centre of pressure approaches the trailing edge when the porosity and the excess length increase as shown in figure 10.

REFERENCES

BARAKAT, R. 1968 Incompressible flow around porous two-dimensional sails and wings. *J. Maths Phys.* **47**, 327–349.

ERDOGAN, F., GUPTA, G. D. & COOK, T. S. 1973 Numerical solution of singular integral equations. In *Method of Analysis and Solution of Crack Problems* (ed. G. C. Shi), pp. 368–425. Noordhoff.

GRADSHTEYN, I. S. & RYZHIK, I. M. 1980 *Tables of Integral Series and Products.* Academic.

MURAI, H. & MARUYAMA, S. 1982 Theoretical investigation of sailwing airfoils taking account of elasticities. *J. Aircraft* **19**, 385–389.

NEWMAN, B. G. & LOW, H. T. 1984 Two-dimensional impervious sails: experimental results compared with theory. *J. Fluid Mech.* **144**, 445–462.

NIELSEN, J. N. 1963 Theory of flexible aerodynamic surfaces. *Trans. ASME* E: *J. Appl. Mech.* **30**, 435–442.

SNEYD, A. D. 1984 Aerodynamic coefficients and longitudinal stability of sail aerofoils. *J. Fluid Mech.* **149**, 127–146.

THWAITES, B. 1961 Aerodynamic theory of sails. *Proc. R. Soc. Lond.* A **261**, 402–422.

VANDEN-BROECK, J.-M. 1982 Nonlinear two-dimensional sail theory. *Phys. Fluids* **25**, 420–422.

VOELZ, K. VAN 1950 Profil und Auftrieb eines Segels. *Z. Angew. Math. Mech.* **30**, 301–317.